To appear in Nature

Wavelike properties of solar supergranulation

L. Gizon*, T. L. Duvall Jr.†, and J. Schou*

** W. W. Hansen Experimental Physics Laboratory, Stanford University, Stanford, CA 94305, USA*

† Laboratory for Astronomy and Solar Physics, NASA Goddard Space Flight Center, Greenbelt, MD 20771, USA

Supergranulation[1,2] on the surface of the Sun is a pattern of horizontal outflows with a distinct scale of 30 Mm and an apparent lifetime of 1 day, outlined by a network of small magnetic features. It is believed that supergranulation corresponds to a preferred cellular scale of thermal convection, and that rising magnetic fields are dragged by the flows and concentrate into ropes at the cell boundaries.[3] However, the solar convection zone is so highly turbulent and stratified that numerical modeling of supergranulation has remained elusive. The dynamics of the supergranulation is not understood and there is no explanation for the observation that the pattern appears to rotate faster[4,5] around the Sun than the magnetic features. Here we report that supergranulation undergoes oscillations and supports waves with periods of 6-9 days. Waves are predominantly prograde, which explains the super-rotation of the pattern. We measure the rotation of the plasma through which the supergranulation pattern propagates and conclude that it is consistent with the motion of the magnetic network.

To study supergranulation, we use a 60-day sequence of Doppler velocity images obtained in 1996 by the Michelson Doppler Imager[6] on board the Solar and Heliospheric Observatory (SOHO). Images are tracked at the Carrington angular velocity ($\Omega_{\rm C} = 2.87$ μrad s^{-1}) to remove the main component of solar rotation. We apply the techniques of time-distance helioseismology[7] to obtain every 12 hr a $120^\circ \times 120^\circ$ map of the horizontal divergence of the flows in a 1 Mm-deep layer beneath the surface.[8] Unlike raw Doppler images, the divergence signal has uniform sensitivity across the solar disk and is subject to few systematic errors. Supergranules appear as cellular patterns of horizontal outward flow in the divergence maps.

For any given target latitude, λ, we extract a longitudinal section of the data 10°-wide in latitude centered about λ. The divergence signal is Fourier transformed in three dimensions to make power spectra as a function of frequency, ν, and horizontal wavevector, $\mathbf{k} = (k_x, k_y)$, where k_x and k_y are in the East-West and South-North directions respectively. In cylindrical coordinates, $\mathbf{k}$ is uniquely specified by its magnitude, k, and its direction, ψ, such that $k_x = k\cos\psi$ and $k_y = k\sin\psi$. Figure 1 shows cuts in the equatorial power spectrum at a constant k typical of the supergranulation. For each azimuth ψ, the power has two broad peaks at frequencies ν_+ and ν_- (Fig. 1a). No Galilean transformation can cause these peaks to coalesce, at zero frequency or otherwise. This implies that the supergranulation undergoes oscillations.

Observations show that the frequencies $\nu_\pm$ have a sinusoidal dependence with ψ of the form $\pm\nu_0 + \nu_1\cos(\psi - \psi_0)$ (Fig. 1b). We interpret ν_1 to be a Doppler frequency shift, $\nu_1 = k\|\mathbf{u}\|/2\pi$, produced by a horizontal background flow $\mathbf{u}$ pointing in the direction ψ_0, as one does in helioseismological ring analysis.[9] The nearly linear relationship measured between ν_1 and k in the range $40 < kR < 180$ is consistent with this interpretation. The latitudinal dependence of $\mathbf{u}$ is shown in Figure 2. The inferred rotation (Fig. 2a) and meridional circulation (Fig. 2b) are both remarkably similar to that of the small magnetic features.[10,11] This property is consistent with the view that magnetic fields are advected by supergranular flows.

The dynamics of the supergranulation is best studied once the background flow, $\mathbf{u}$, has been removed. In a co-moving frame, each spatial component oscillates at a characteristic frequency ν_0. We find a clear relationship between ν_0 and the wavenumber k, well described by a power law (Fig. 3a). This is a fundamental relationship as it is measured to be independent of both ψ and λ. The data are consistent with a spectrum of travelling waves with a dispersion relation $\nu = \nu_0(k)$. The waves have a rather low quality factor, as can be seen in the azimuthally averaged power spectrum (Fig. 3b).

Since ν_0 and the dominant size[12] of supergranules are observed to be essentially independent of latitude, the general dynamics determining the time scale and the spatial scale of supergranulation is not affected by the Coriolis force associated with the large scale vorticity (rotation). We observe, however, a pronounced anisotropy in the azimuthal distribution of wave power at fixed k (Fig. 4a). The power is maximum in the direction of rotation and toward the equator in both hemispheres (Fig. 4b). The pattern therefore senses the effect of rotation. A snapshot of the divergence field would not reveal this as the sum of the powers measured in opposite directions is isotropic (Fig. 4a); the vorticity field, on the other hand, is known[8] to be slightly sensitive to the effect of the Coriolis force.

Earlier estimates[4,5] of the supergranulation rotation, obtained by tracking the supergranulation pattern from one image to the next, were systematically found to be higher[13] than the rotation of the magnetic network (Fig. 2a). This apparent super-rotation of the pattern can now be understood since waves are predominantly prograde. The East-West motion of the pattern is effectively a power-weighted average of the true rotation and the non-advective phase speed $u_{\rm w} = 2\pi\nu_0/k \sim 65\ {\rm m\,s^{-1}}$. Similarly, the excess of wave power toward the equator is reflected in the meridional motion of the pattern (Fig. 2b).

We have shown that supergranulation displays a high level of organization in space and time. It is known[14] that heat and momentum transport in turbulent rotating convection is controlled by a network of coherent cyclonic plumes sinking from the thermal boundary layer. These plumes may be at the origin of the organization of the supergranulation pattern. We find that supergranulation supports waves. The prograde excess of wave power is most likely due to the influence of rotation that breaks the East-West symmetry, allowing for new instabilities to propagate. Recent numerical simulations[15] of solar convection show convective patterns that move prograde relative to the local rotation at low latitudes, and may help explain the observations. Convection in oblique magnetic fields[16] also exhibits solutions that take the form of travelling waves, where the tilt of the convection cells, their wave speed, and direction depend on the strength and obliquity of the field. Supergranulation would appear to be a rare known example of travelling wave convection in a very highly turbulent fluid, a non-linear phenomenon which has been observed in laboratory and numerical experiments[15–18] under much weaker conditions of turbulence. We suggest that supergranular waves may be used as a diagnostic tool for probing the upper solar convection zone.

References

1. Leighton, R. B., Noyes, R. W. & Simon, G. W. Velocity fields in the solar atmosphere. I. Preliminary report. *Astrophys. J.* **135**, 474-499 (1962).

2. Simon, G. W. & Leighton, R. B. Velocity fields in the solar atmosphere. III. Large-scale motions, the chromospheric network, and magnetic fields. *Astrophys. J.* **140**, 1120-1147 (1964).

3. Galloway, D. J. & Weiss, N. O. Convection and magnetic fields in stars. *Astrophys. J.* **243**, 945-953 (1981).

4. Duvall, T. L., Jr. The equatorial rotation rate of the supergranulation cells. *Sol. Phys.* **66**, 213-221 (1980).

5. Snodgrass, H. B. & Ulrich, R. K. Rotation of Doppler features in the solar photosphere. *Astrophys. J.* **351**, 309-316 (1990).

6. Scherrer P. H. *et al.* The Solar Oscillations Investigation - Michelson Doppler Imager. *Sol. Phys.* **162**, 129-188 (1995).

7. Duvall, T. L., Jr. *et al.* Time-distance helioseismology. *Nature* **362**, 430-432 (1993).

8. Duvall, T. L., Jr., & Gizon, L. Time-distance helioseismology with f modes as a method for measurement of near-surface flows. *Sol. Phys.* **192**, 177-191 (2000).

9. Schou, J. & Bogart, R. S. Flow and horizontal displacements from ring diagrams. *Astrophys. J.* **504**, L131-134 (1998).

10. Komm R. W., Howard R. F. & Harvey J. W. Rotation rates of small magnetic features from two- and one-dimensional cross-correlation analyses. *Sol. Phys.* **145**, 1-10 (1993).

11. Komm R. W., Howard R. F. & Harvey J. W. Meridional flow of small photospheric magnetic features. *Sol. Phys.* **147**, 207-223 (1993).

12. Beck, J. G. *Large Scale Solar Velocities on Time Scales up to Thirty Days.* Thesis, Univ. California (1997).

13. Beck, J. G. & Schou, J. Supergranulation rotation. *Sol. Phys.* **193**, 333-343 (2000).

14. Brummell, N. H., Hurlburt, N. E. & Toomre, J. Turbulent compressible convection with rotation. I. Flow structure and evolution *Astrophys. J.* **473**, 494-513 (1996).

15. Miesch, M. S. et al. three-dimensional spherical simulations of solar convection. I. Differential rotation and pattern evolution achieved with laminar and turbulent states. *Astrophys. J.* **532**, 593-615 (2000)

16. Hurlburt, N. E., Matthews, P. C. & Proctor, M. R. E. Nonlinear compressible convection in oblique magnetic fields. *Astrophys. J.* **457**, 933-938 (1996).

17. Zhong, F., Ecke, R. & Steinberg, V. Asymmetric modes and the transition to vortex structures in rotating Rayleigh-Bénard convection. *Phys. Rev. Lett.* **67**, 2473-2476 (1991).

18. Walden, R. W. *et al.* Traveling waves and chaos in convection in binary fluid mixtures. *Phys. Rev. Lett.* **55**, 496-499 (1985).

Acknowledgments

Special thanks are due to D. O. Gough for suggestions about the general presentation of the paper. We also thank P. Milford, P. H. Scherrer, C. J. Schrijver, and N. O. Weiss for useful comments. SOHO is a mission of international cooperation between the European Space Agency and NASA. MDI is supported by the Office of Space Sciences of NASA.

Correspondence and requests for material should be addressed to L.G.
(e-mail: lgizon@solar.stanford.edu).

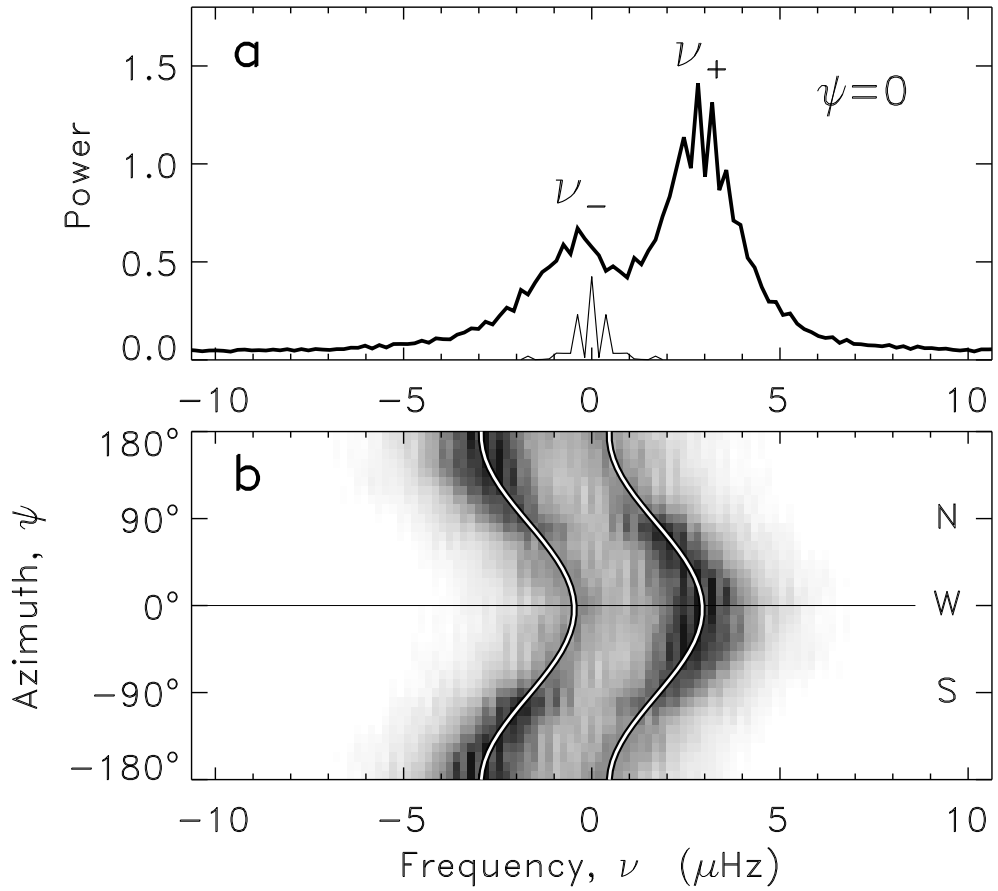

Figure 1 Power spectrum of the supergranulation signal near the equator ($\lambda = 0°$). Cuts are shown at constant wavenumber $k = 120/R$ where R is the solar radius. **a**, The thick line is the power spectrum versus frequency, ν, for $\mathbf{k} = (k, 0)$ pointing in the direction of solar rotation, $\psi = 0$ (West). There are two peaks at frequencies ν_- and ν_+. The frequency resolution is given by the power spectrum of the temporal window function (thin line). **b**, Cylindrical cut, $P_k(\nu, \psi)$, in the power spectrum at constant k versus ν and the direction of $\mathbf{k}$, ψ. By construction, $P_k(\nu, \psi) = P_k(-\nu, \psi - \pi)$. Power peaks in two ridges at frequencies $\nu_-(\psi)$ and $\nu_+(\psi)$. For each ψ, we measure $\nu_\pm$ by fitting the sum of two independent Lorentzian functions to the power. The fits take into account the convolution by the window function. The sinusoidal variation of $\nu_\pm$ with ψ is due to advection by a background flow $\mathbf{u} = (u_x, u_y)$. The double lines show the fit $\nu = \pm\nu_0 + (ku_x \cos\psi + ku_y \sin\psi)/2\pi$ to $\nu_\pm(\psi)$, where ν_0 is a constant frequency. At the equator we find $\mathbf{u} = (43, 0)$ m s^{-1}. The velocity u_x is measured in a frame co-rotating with the Sun at the Carrington rotation rate.

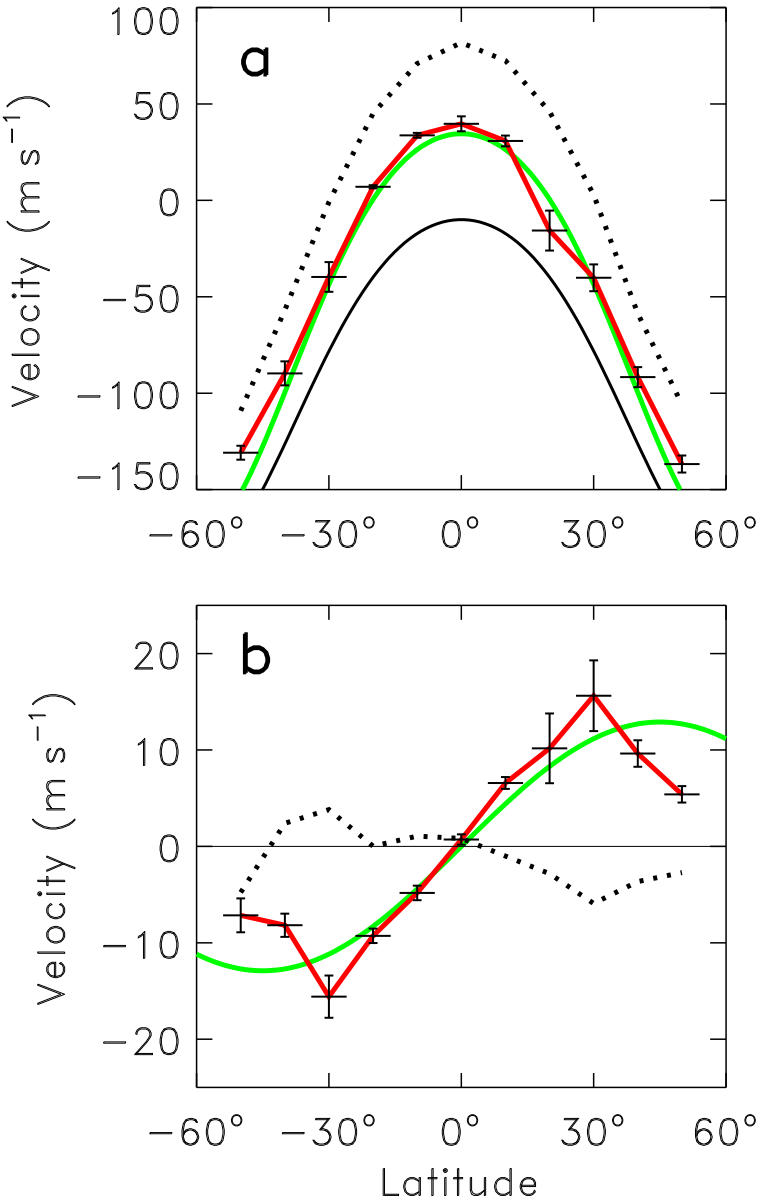

Figure 2 Flows, **u**, inferred from the advection of the supergranulation versus latitude, λ. **a**, Flow in the direction of solar rotation, u_x (red). The green line shows the rotation of the small magnetic features[10] and the black line is for the photospheric rotation.[5] The dotted line shows the pattern rotation obtained by tracking supergranular features with a 24 hr delay, in agreement with an earlier measurement.[5] **b**, Northward meridional flow, u_y (red). The meridional flow of the magnetic features[11] (green) is again similar. The dotted line shows the anomalous results obtained by tracking the supergranulation pattern with a 24 hr delay.

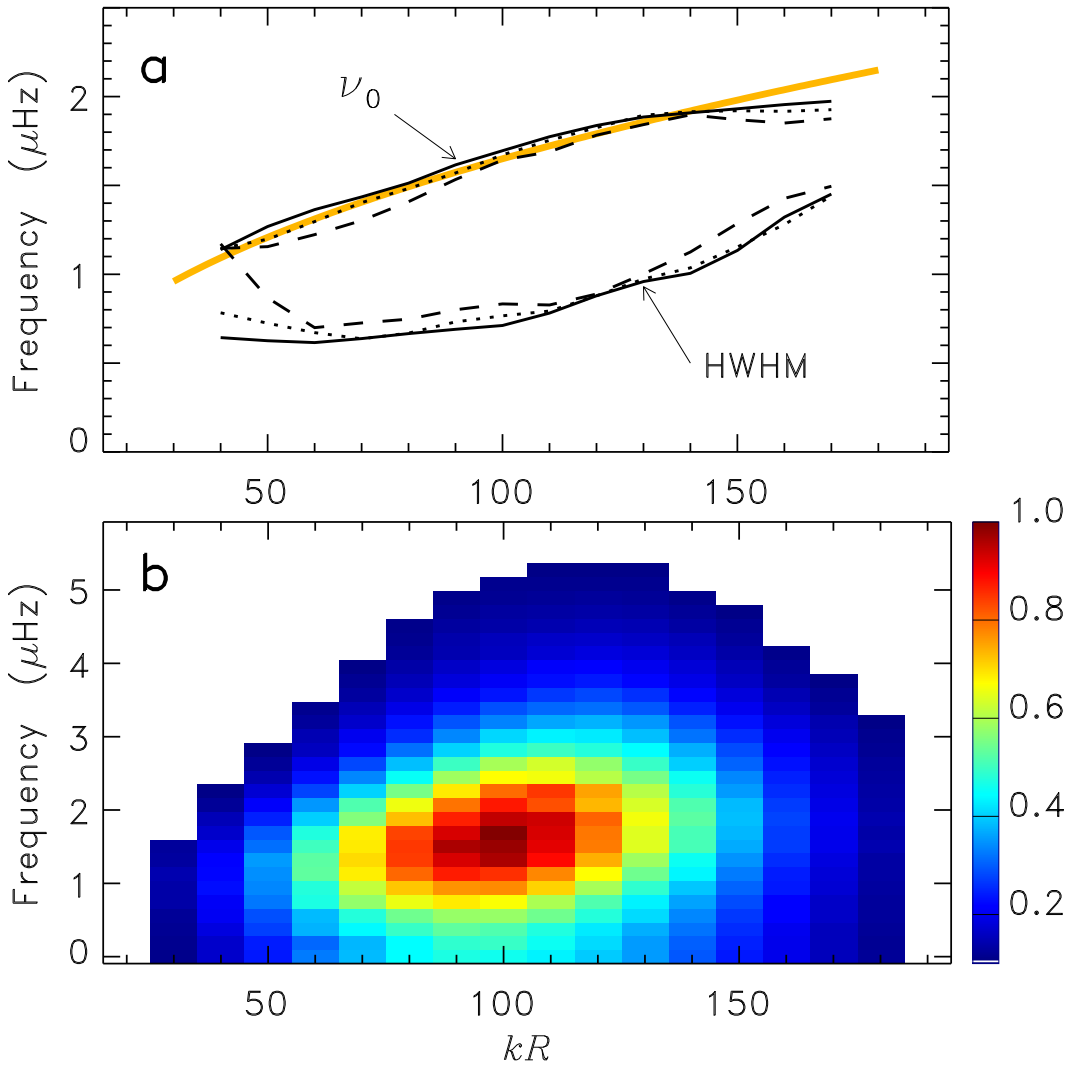

Figure 3 Average dynamical properties in a co-moving frame. **a**, Oscillation frequency ν_0 versus kR at latitudes $\lambda = 0°$ (solid), $\lambda = \pm 25°$ (dotted) and $\lambda = \pm 50°$ (dashed). For reference, we plot the approximate dispersion relation $\nu = 1.65(kR/100)^{0.45}$ μHz (orange). Also shown is the half width at half maximum (HWHM) of the Lorentzian profiles for the same latitudes, implying an e-folding lifetime of 1-3 days. The quality factor, ν_0/HWHM, does not exceed 2. **b**, Power spectrum corrected for rotation and meridional circulation and averaged over azimuth and latitude. We note that the distribution of power as a function of frequency is affected only by the known temporal window function, while the wavenumber dependence includes effects of the telescope optics and of the time-distance analysis which are not fully understood.

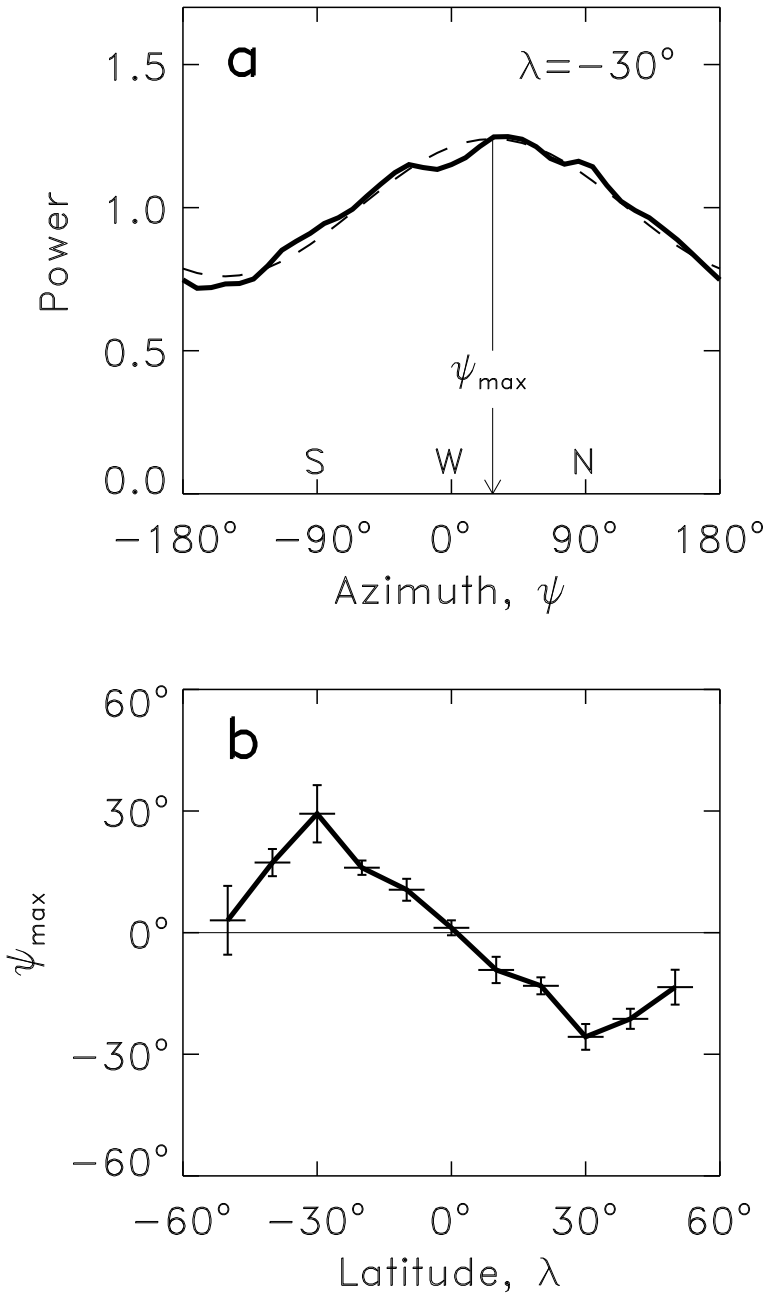

Figure 4 Wave power as a function of azimuth and latitude. **a**, Directional distribution of power at latitude $\lambda = -30°$ (solid line), obtained by integrating $P_k(\nu, \psi)$ over frequencies $\nu > \mathbf{k} \cdot \mathbf{u}/2\pi$ and then averaging over k. We applied an MTF correction estimated from the data. The azimuth of maximum power, $\psi_{\max}$, is measured by fitting a sinusoidal function (dashed line). **b**, Plot of $\psi_{\max}$ versus latitude.